

# Pharmacogenetics-based population pharmacokinetic analysis of etravirine in HIV-1 infected individuals

Rubin Lubomirov<sup>a,\*</sup>, Mona Arab-Alameddine<sup>b,i,\*</sup>, Margalida Rotger<sup>a,\*</sup>, Aurélie Fayet-Mello<sup>b</sup>, Raquel Martinez<sup>a</sup>, Monia Guidi<sup>b,i</sup>, Julia di Iulio<sup>a</sup>, Matthias Cavassini<sup>c</sup>, Huldrych F. Günthard<sup>d</sup>, Hansjakob Furrer<sup>e</sup>, Catia Marzolini<sup>f</sup>, Enos Bernasconi<sup>g</sup>, Alexandra Calmy<sup>h</sup>, Thierry Buclin<sup>b</sup>, Laurent A. Decosterd<sup>b</sup>, Chantal Csajka<sup>b,i</sup>, Amalio Telenti<sup>a</sup> and the Swiss HIV Cohort Study

**Objectives** Etravirine (ETV) is metabolized by cytochrome P450 (CYP) 3A, 2C9, and 2C19. Metabolites are glucuronidated by uridine diphosphate glucuronosyltransferases (UGT). To identify the potential impact of genetic and non-genetic factors involved in ETV metabolism, we carried out a two-step pharmacogenetics-based population pharmacokinetic study in HIV-1 infected individuals.

**Materials and methods** The study population included 144 individuals contributing 289 ETV plasma concentrations and four individuals contributing 23 ETV plasma concentrations collected in a rich sampling design. Genetic variants [ $n=125$  single-nucleotide polymorphisms (SNPs)] in 34 genes with a predicted role in ETV metabolism were selected. A first step population pharmacokinetic model included non-genetic and known genetic factors (seven SNPs in *CYP2C*, one SNP in *CYP3A5*) as covariates. Post-hoc individual ETV clearance (CL) was used in a second (discovery) step, in which the effect of the remaining 98 SNPs in *CYP3A*, *P450 cytochrome oxidoreductase (POR)*, nuclear receptor genes, and *UGTs* was investigated.

**Results** A one-compartment model with zero-order absorption best characterized ETV pharmacokinetics. The average ETV CL was 41 (l/h) (CV 51.1%), the volume of distribution was 1325 l, and the mean absorption time was 1.2 h. The administration of darunavir/ritonavir or tenofovir was the only non-genetic covariate influencing ETV CL significantly, resulting in a 40% [95% confidence interval (CI): 13–69%] and a 42% (95% CI: 17–68%) increase in ETV CL, respectively. Carriers of rs4244285 (*CYP2C19\*2*) had 23% (8–38%) lower ETV CL.

## Introduction

Etravirine (ETV) is a non-nucleoside reverse transcriptase inhibitor active against HIV. It is recommended at a dose of 200 mg twice daily, with maximum concentrations

Co-administered antiretroviral agents and genetic factors explained 16% of the variance in ETV concentrations. None of the SNPs in the discovery step influenced ETV CL.

**Conclusion** ETV concentrations are highly variable, and co-administered antiretroviral agents and genetic factors explained only a modest part of the interindividual variability in ETV elimination. Opposing effects of interacting drugs effectively abrogate genetic influences on ETV CL, and vice-versa. *Pharmacogenetics and Genomics* 23:9–18 © 2012 Wolters Kluwer Health | Lippincott Williams & Wilkins.

*Pharmacogenetics and Genomics* 2013, 23:9–18

**Keywords:** *CYP2C9*, *CYP2C19*, etravirine, HIV-infected individuals, NONMEM, pharmacogenetics, pharmacokinetics

<sup>a</sup>Institute of Microbiology, <sup>b</sup>Division of Clinical Pharmacology and Toxicology, <sup>c</sup>Division of Infectious Diseases, University Hospital Center, University of Lausanne, Lausanne, <sup>d</sup>Division of Infectious Diseases and Hospital Epidemiology, University Hospital Zurich, University of Zurich, Zurich, <sup>e</sup>Division of Infectious Diseases, University Hospital and University of Bern, Bern, <sup>f</sup>Division of Infectious Diseases and Hospital Epidemiology, University Hospital Basel, Basel, <sup>g</sup>Division of Infectious Diseases, Regional Hospital of Lugano, Lugano, <sup>h</sup>HIV Unit, Division of Infectious Diseases, University Hospital Geneva and <sup>i</sup>School of Pharmacy, Department of Pharmaceutical Sciences, University of Lausanne and Geneva, Geneva, Switzerland

Correspondence to Amalio Telenti, MD, Institute of Microbiology, University Hospital Center (CHUV), Bugnon 48, 1011 Lausanne, Switzerland  
Tel: +41 21 314 05 50; fax: +41 21 314 40 95; e-mail: amalio.telenti@chuv.ch

Present address: Rubin Lubomirov, Clinical Pharmacology Center, Department of Pharmacology and Therapeutics, La Paz University Hospital, School of Medicine, Autonomous University of Madrid, IdiPAZ, Madrid, Spain.

\*Rubin Lubomirov, Mona Arab-Alameddine, and Margalida Rotger contributed equally to the work.

Received 4 June 2012 Accepted 28 September 2012

Supplemental digital content is available for this article. Direct URL citations appear in the printed text and are provided in the HTML and PDF versions of this article on the journal's Website ([www.pharmacogeneticsandgenomics.com](http://www.pharmacogeneticsandgenomics.com)).

1744-6872 © 2012 Wolters Kluwer Health | Lippincott Williams & Wilkins

DOI: 10.1097/FPC.0b013e32835ade82

diphosphate glucuronosyltransferases (UGT). The UGT isoenzymes responsible are currently unknown [2,3]. ETV has been shown to be a weak inducer of CYP3A4 and a weak inhibitor of CYP2C9 and CYP2C19 [2–4], and does not seem to be a substrate for ABC transporters [3,5]. ETV exposure is characterized by high interindividual variability explained in part by interactions with food intake and other medications [4,6–8]; however, the contribution of host genetic factors is currently unknown.

We carried out a two-step pharmacogenetics-based population pharmacokinetic study of ETV in HIV-1 infected individuals. The first step aimed to build up a population pharmacokinetic model to describe the disposition of ETV, assess its variability, and identify and quantify the contribution of demographic factors as well as functional variants of well-known genes involved in ETV metabolism (*CYP2C* and *CYP3A* locus). A second discovery step aimed to identify new candidate variants in *CYP3A*, *P450 cytochrome oxidoreductase* (*POR*), nuclear receptors, and *UGT* isoenzymes likely to affect ETV disposition. A candidate variant was brought to validation in an independent set of study participants.

## Materials and methods

### Population and study design

This study was carried out within the framework of the Swiss HIV Cohort Study (<http://www.shcs.ch>). The ethics committees of all participating centers approved the project and all participants provided written informed consent for genetic testing. Initially, 148 HIV-infected individuals were included in the study: 144 individuals were recruited through therapeutic drug monitoring (TDM) between January 2008 and November 2009 and provided 289 ETV plasma concentrations. All individuals signed genetic consent. Four individuals were recruited through an open-label prospective study to measure the cellular disposition of the integrase inhibitor raltegravir [9] and contributed 23 ETV plasma concentrations collected in a rich sampling design.

### Analytical method

Plasma samples obtained from HIV-infected individuals were isolated by centrifugation and stored at  $-20^{\circ}\text{C}$  until batch analysis. On the day of the analysis, samples were inactivated for virus at  $60^{\circ}\text{C}$  for 60 min. Plasma ETV levels were determined by high-performance liquid chromatography coupled with tandem mass spectrometry (LC-MS/MS) after protein precipitation with acetonitrile according to our previously reported analytical method [10]. The high-performance liquid chromatography system was a Rheos 2200 binary pump (Flux Instruments, Basel, Switzerland) equipped with an online degasser and a temperature-controlled 324 vial autosampler maintained at  $+10^{\circ}\text{C}$  (CTC Analytics AG, Zwingen, Switzerland). The chromatographic system was coupled to a triple-stage quadrupole mass spectrometer (TSQ

Quantum Discovery; Thermo Electron Corporation, Waltham, Massachusetts, USA) equipped with an electrospray ionization interface operated in the positive ion mode and controlled with the Xcalibur 1.1 software (Thermo Electron Corporation, San Jose, California, USA). The selected mass transitions for ETV were  $m/z$  434.9  $\rightarrow$  303. The method was validated according to the recommendations published online by the Food and Drugs Administration (FDA) [11]. The method was precise and accurate within the range of calibration (10–4000 ng/ml) with interassay precision (CV%) and accuracy (bias%) for the low-quality, medium-quality, and high-quality control plasma samples (100, 500, and 3000 ng/ml, respectively) ranging between 6.9 and 8.1% and  $-3.3$  and  $3.5\%$ , respectively. The calibration curves are linear, with a lower limit of quantification of 10 ng/ml. The laboratory participates in an international external quality assurance program for antiretroviral drugs analysis (KKGIT, *Stichting Kwaliteitsbewaking Klinische Geneesmiddelenanalyse en Toxicologie*, Association for Quality Assessment in TDM and clinical Toxicology, the Hague, the Netherlands).

### Genotyping

The two-step study design to estimate the impact of genetic variants on ETV pharmacokinetics was as follows: the first assessment step included functional single-nucleotide polymorphisms (SNPs) in genes relevant to ETV metabolism (*CYP2C8*, *CYP2C9*, *CYP2C19*, and *CYP3A5*), whereas the second discovery step included SNPs in genes possibly relevant for ETV metabolism (*CYP3A*, *POR*, nuclear receptors, and *UGTs*). For this purpose, we selected 125 SNPs representing common genetic variation enriched by variants with a proven functional effect in a total of 34 genes in Caucasians. Genotyping was carried out using a 120-plex customized Veracode microarray (Illumina, Eindhoven, the Netherlands). The complete list of genes and SNPs included in the array is shown in Supplementary Table S1 (<http://links.lww.com/FPC/A534>). SNPs that were not included in the array because of technical limitations ( $n = 5$ ) were genotyped either by TaqMan allelic discrimination (Applied Biosystems, Foster City, California, USA) (*POR*\*28 [rs1057868]) or by direct sequencing (*UGT1A3*\*2b [rs3821242, rs6431625] and *UGT1A1*\*28 [rs8175347]). *UGT2B17* gene deletion was investigated using a previously published PCR strategy [12] (Supplementary Table S2, <http://links.lww.com/FPC/A535>). Functional polymorphisms were obtained from the literature ( $n = 65$ ). In summary, we included five SNPs in *CYP2C19* and four SNPs in *CYP2C9* proven functional SNPs in genes confirmed to be involved in ETV metabolism [13–18]. Although *CYP3A* is directly involved in ETV metabolism, we only considered *CYP3A5*\*3 (rs776746) as a proven functional variant; other SNPs in *CYP3A* were included as candidate SNPs in the discovery step because of insufficient support for a functional role of specific

variants [19,20] (Table 1). Similarly, although various SNPs in *UGTs* and nuclear receptor genes are functional variants, they were also considered in the discovery step because their effect on ETV metabolism is unknown. Tagging SNPs (tSNPs) were selected on the basis of HapMap Phase III data (release 24) (<http://www.hapmap.org>) using Tagger software [21] to capture SNPs with minor allelic frequency greater than 5% in the HapMap CEU population with the mean maximum pairwise  $R^2$  between tSNPs and not genotyped SNPs of 0.80. The tSNPs ( $n = 52$ ) were selected to cover the RefSeq genes' longest transcript plus 5 kb at the 3' and 5'-UTR region in the HapMap Genome Browser (<http://www.hapmap.org>). Haplotype tagging SNPs (htSNPs,  $n = 8$ ) were selected to better cover the allelic diversity of the locus *UGT1A* [22]. Genotyping quality control was ensured by (i) including duplicated samples in all array plates, (ii) removing SNPs that failed in more than 5% of samples, (iii) removing SNPs that departed from Hardy-Weinberg equilibrium ( $P < 0.001$ ) [23], and (iv) keeping genotyping blind with respect to the phenotype. SNPs that failed in the array (rs1799853, rs1057910, rs7643645) were genotyped by commercially available TaqMan allelic discrimination. For replication, the candidate SNP identified through the array analysis (rs2003569) was genotyped using TaqMan allelic discrimination (Supplementary Table S2). Genotyping was completed for 144 individuals. An independent set of 64 individuals recruited through TDM between December 2009 and September 2010 was included in a validation sample of the rs2003569 marker.

## Population pharmacokinetic model (Pop-PK)

### Basic model

A stepwise procedure was used to find the model that fitted ETV data the best. First, one-compartment and two-compartment models with first-order and zero-order absorption were tested. The best structural model appeared to be a one-compartment model with zero-order absorption and linear elimination from the gastrointestinal tract. The estimated parameters were clearance ( $CL$ ), volume of distribution ( $V_d$ ), and the duration of absorption ( $D_1$ ). As ETV was only administered orally,  $CL$

and  $V_d$  represent apparent values ( $CL/F$  and  $V_d/F$ , respectively, where  $F$  is the absolute oral bioavailability).

### Statistical model

Exponential errors following a log-normal distribution were assumed for the description of the interindividual variability in the pharmacokinetic parameters as shown by the equation  $\theta_j = \theta e^{\eta_j}$ , where  $\theta_j$  is the individual pharmacokinetic parameter of the  $j$ th individual,  $\theta$  is the geometric average population value, and  $\eta_j$  is the random-effect value, which is an independent, normally distributed effect with a mean of 0 and a variance of  $\Omega$ . A proportional error model was assigned to the intraindividual (residual) variability.

### Demographic covariates model

Graphical explorations of covariates effect were first carried out and potentially influential covariates were incorporated sequentially into the pharmacokinetic model. On the basis of these relationships, the typical values of the pharmacokinetic parameters were modeled to depend linearly on a covariate  $X$  (centered on the mean for demographic covariates) using  $CL = \theta_a(1 + \theta_b X)$ , where  $\theta_a$  is the average estimate and  $\theta_b$  is the relative deviation from the average attributed to the covariate  $X$ , or using  $CL = \theta_a(\theta_b)^X$  for binary covariates. The available covariates were sex, ethnicity, age, body weight, height, comedication, laboratory markers of hepatic function, bilirubin, aspartate transferases and amino alanine transferases, and hepatitis C coinfection. Food intake was not recorded.

### Genetic covariates model

All proven functional SNPs in *CYP2C8*, *CYP2C9*, and *CYP2C19*, and the best-characterized functional SNP in the *CYP3A* locus (*CYP3A5*\*3) were included in the model as covariates. Individuals were categorized into three genetic groups: homozygous for the common alleles (Ref), heterozygous loss of function (Het LOF), and homozygous (Hom LOF) for the rare allele. Gain-of-function (GOF) allele *CYP2C19*\*17 individuals were categorized into Ref, Het GOF, and Hom GOF. A rich

**Table 1** Proven functional single-nucleotide polymorphisms in *CYP2C8*, *CYP2C9*, *CYP2C19*, and *CYP3A5* included in the model

Gene	rs number	Allele name	Allele change	Effect minor allele	Minor allelic frequency (95% CI)
<i>CYP2C19</i>	rs12248560	<i>CYP2C19</i> *17	C>T	GOF	0.155 (0.116–0.204)
<i>CYP2C19</i>	rs28399504	<i>CYP2C19</i> *4	A>G	LOF	0
<i>CYP2C19</i>	rs41291556	<i>CYP2C19</i> *8	T>C	LOF	0
<i>CYP2C19</i>	rs4244285	<i>CYP2C19</i> *2	G>A	LOF	0.178 (0.137–0.229)
<i>CYP2C19</i>	rs72558186	<i>CYP2C19</i> *7	T>A	LOF	0
<i>CYP2C9</i>	rs1799853	<i>CYP2C9</i> *2	C>T	DOF	0.101 (0.07–0.143)
<i>CYP2C9</i>	rs28371685	<i>CYP2C9</i> *11	C>T	DOF	0.007 (0.001–0.028)
<i>CYP2C9</i>	rs1057910	<i>CYP2C9</i> *3	A>C	DOF	0.066 (0.041–0.103)
<i>CYP2C9</i>	rs9332239	<i>CYP2C9</i> *12	C>T	DOF	0.007 (0.001–0.028)
<i>CYP2C8</i>	rs10509681	<i>CYP2C8</i> *3	T>C	DOF	0.104 (0.073–0.147)
<i>CYP3A5</i>	rs776746	<i>CYP3A5</i> *3	T>C	LOF	0.840 (0.792–0.880)

CI, confidence interval; DOF, decrease of function; GOF, gain of function; LOF, loss of function.

model was defined as the one where Ref, Het, and Hom were allowed to have distinct values for CL. A reduced model was defined either as dominant when the Het and Hom were grouped and allowed to have a single value for CL, or as recessive when only Hom had a distinct CL value.

### Parameter estimation and selection

Data analysis was carried out with NONMEM (version VII, NM-TRAN version II) [24] using the first-order conditional estimation method with interaction. As a goodness-of-fit statistic, NONMEM uses an objective function, which is approximately equal to minus twice the logarithm of the maximum likelihood. The likelihood ratio test, on the basis of the reduction in the objective function ( $\Delta OF$ ), was used to compare two models. A  $\Delta OF$  ( $-2 \log$  likelihood, approximate  $\chi^2$ -distribution) of 3.84, 5.99, 7.81, and 9.48 points for 1, 2, 3, or 4 additional parameters, respectively, was used to determine statistical significance ( $P < 0.05$ , two-sided) between two models. Covariate analysis involved forward selection of influential factors, followed by backward deletion. Model assessment was carried out on the basis of diagnostic plots [goodness-of-fit plots and visual predictive checks (VPCs)], along with the measure of the SEs, correlation matrix of parameter estimates, and the size of residual errors.

### Model evaluation and assessment

The reliability of the analysis results was determined using a bootstrap resampling procedure with replacement on 200 replicates. The median and 95% confidence interval (CI) of each parameter were compared with those estimated from the original dataset. The statistical analysis was carried out using Perl-speaks-NONMEM, version 3.2.4 (<http://psn.sourceforge.net>). In addition, an independent set of 88 individuals recruited through TDM between September 2010 and October 2011 was used for external model validation. The accuracy and precision of the model were assessed, respectively, by the mean prediction error and the root mean squared error [25]. A sensitivity analysis was carried out to account for potential compliance issues associated with low drug levels. Individuals under treatment for more than 3 months with either viral load greater than 50 copies/mm<sup>3</sup> and concentrations below the 10th percentile of the expected concentrations over the dosing interval, or with greater than 400 copies/mm<sup>3</sup> were excluded from the analysis. Robustness of the estimates of the final model with and without these individuals ( $n = 8$ ) was compared. VPC was carried out using NONMEM by simulations on the basis of the final pharmacokinetic estimates for the most frequent dosage regimens (200 mg twice daily and 400 mg once daily) using 1000 individuals to calculate 95% prediction intervals. The concentrations encompassing the range from 2.5th to 97.5th percentiles at each time point were retrieved to construct the intervals.

### Genetic discovery analysis

The genetic association analysis examined the effect of the SNPs in *CYP3A*, *POR*, nuclear receptors, and *UGTs* genes using PLINK [26] with the post-hoc maximum a posteriori Bayesian ETV CL obtained from the final Pop-PK. We explored three different models of phenotypic expression: additive, recessive, and dominant.

## Results

### Population pharmacokinetic (Pop-PK) models

A total of 289 ETV plasma concentrations were obtained from 148 HIV-infected individuals and included in the population pharmacokinetic analysis. Most of the patients received the standard dosing regimen of 200 mg twice daily (51%), 37% of the patients received 400 mg once daily, and 15% received alternative dosing regimens (50, 100, 250, 300, 500, and 800 mg given once or twice daily). ETV concentration measurements were between 4 and 2198 ng/ml. The demographic characteristics of the study population are presented in Table 2.

### Basic model

A one-compartment model with zero-order absorption from the gastrointestinal tract fitted the data best. The use of a first-order model could describe the data equally well, but the absorption rate constant was estimated very imprecisely and was therefore not chosen. Sequential zero-order and first-order absorption models did not significantly improve the fit ( $\Delta OF = 0.0$ ). No further reduction in objective function was observed upon assignment of lag time either ( $\Delta OF = -0.0$ ). Between-participant variability was assigned to CL, but no variability could be found in  $V_d$  or in the duration of the absorption parameter ( $D_1$ ) ( $\Delta OF = -0.0$ ). A proportional error model adequately described the residual error, whereas the use of a combined proportional and additive error model did not improve the description of the data ( $\Delta OF = -0.0$ ). The final population parameters without covariates were a CL of 41 l/h (CV: 51%), a  $V_d$  of 1325 l, and a  $D_1$  of 2.9 h.

### Demographic covariates model

None of the demographic covariates (age, sex, body weight, or ethnicity), hepatitis C coinfection, or any markers of hepatic function, or comedication significantly affected ETV CL. The concomitant administration of ritonavir-boosted darunavir (DRVr) ( $\Delta OF = -16.0$ ,  $P < 0.0001$ ) and tenofovir (TDF) ( $\Delta OF = -22$ ,  $P < 0.0001$ ) significantly influenced ETV CL, resulting in a 40% (95% CI: 13–69%) and a 42% (95% CI: 17–68%) increase in ETV CL, respectively. A similar trend was observed with the coadministration of ritonavir-boosted lopinavir (LPVr), where ETV CL was increased by 40% (95% CI: -11 to 89%), and yet, this effect did not reach statistical significance ( $\Delta OF = -3.4$ ,  $P = 0.06$ ). The two interacting drugs DRVr and TDF decreased the variability in ETV CL by 13%. An additive effect of both DRVr and

**Table 2** Baseline demographics of the study and validation populations

Characteristics	<i>n</i> (%) or median (range)	
	Study population ( <i>n</i> = 148)	Validation set ( <i>n</i> = 88)
Sex (male)	117 (79%)	67 (76%)
Age (years)	46 (16–70)	49 (25–69)
Body weight (kg)	73 (37–110)	72 (46–151)
Height (cm)	173 (152–203)	174 (148–200)
Ethnicity		
Caucasian	132 (89.2%)	73 (83.0%)
African	13 (8.8%)	9 (10.2%)
Asian	2 (1.4%)	3 (3.4%)
Unknown	1 (0.7%)	3 (3.4%)
Viral load (log <sub>10</sub> copies/ml)	1.7 (1.7–5.2)	2.6 (1.3–4.9)
CD4 cell count (cells/μl)	370 (18–1338)	498 (60–1707)
Protease Inhibitors		
Darunavir	69 (46.6%)	37 (42.0%)
Lopinavir	11 (7.4%)	4 (4.5%)
Atazanavir	1 (0.67%)	5 (5.7%)
Fosamprenavir	1 (0.67%)	–
Nucleoside/nucleotide reverse transcriptase inhibitors		
Tenofovir	87 (58.8%)	50 (56.8%)
Emtricitabine	2 (1.35%)	38 (43.2%)
Lamivudine	57 (38.5%)	19 (21.6%)
Abacavir	1 (0.67%)	–
Zidovudine	12 (8.1%)	–
Didanosine	3 (2.0%)	1 (1.1%)
Entry inhibitors		
Maraviroc	12 (8.1%)	3 (3.4%)
Enfuvirtide	4 (2.7%)	2 (2.2%)
Integrase inhibitors		
Raltegravir	64 (43.2%)	39 (44.3%)
Non-ART interacting drugs		
Sulfamethoxazole-trimethoprim	26 (17.5%)	1 (1.1%)
Pantoprazole	7 (4.7%)	2 (2.2%)
Rabeprazole	2 (1.3%)	–
Esomeprazole	5 (3.37%)	2 (2.2%)
Fluconazole	1 (0.3%)	–
Omeprazole	2 (1.3%)	–
Itraconazole	1 (0.3%)	–
Carbamazepine	1 (0.3%)	–
Other antiacids	1 (0.3%)	–
Isoniazid	1 (0.3%)	2 (2.2%)
HCV coinfection	28 (18.9%)	21 (23.9%)
rs4244285 ( <i>CYP2C19</i> *2) <sup>a</sup>		Not done
GG	96 (67%)	
GA	43 (30%)	
AA	4 (2%)	
Not working	1 (1%)	
rs1057910 ( <i>CYP2C9</i> *3) <sup>a</sup>		Not done
GG	126 (87%)	
GA	17 (12%)	
AA	1 (1%)	

ART, antiretroviral therapy.

<sup>a</sup>Genotyping missing for four individuals.

TDF on ETV exposure was observed, yielding a 100% increase in ETV CL. Yet, no hypersynergistic effect was detected.

### Genetic covariates model

Among the 11 proven functional SNPs in *CYP2C8*, *CYP2C9*, *CYP2C19*, and *CYP3A5* (Table 1), three were found to be monomorphic [rs28399504 (*CYP2C19*\*4), rs72558186 (*CYP2C19*\*7), and rs41291556 (*CYP2C19*\*8)]; thus, eight SNPs were included in the model. rs4244285

(*CYP2C19*\*2) was found to improve the model significantly ( $\Delta\text{OF} = -8.34$ ,  $P = 0.003$ ). No significant difference in CL was observed between Het LOF or Hom LOF ( $\Delta\text{OF} = -2$ ) owing to the low number ( $n = 4$ ) of homozygous individuals. LOF carriers of rs4244285 (*CYP2C19*\*2) showed a 23% (95% CI: 8–38%) decrease in ETV CL, and explained 5% of the variability in CL. A similar effect was observed in LOF carriers of rs1057910 (*CYP2C9*\*3), indicating a 21% (95% CI: –6.8 to 48.3%) lower ETV CL compared with Ref allele carriers. This influence did not reach statistical significance, although ( $\Delta\text{OF} = -2.5$ ,  $P = 0.1$ ), and did not explain between-participant variability in CL. Gain-of-function allele rs12248560 (*CYP2C19*\*17) and loss-of-function allele rs776746 (*CYP3A5*\*3) were not associated with ETV CL.

Multivariate analyses and backwards deletion confirmed that DRVr and TDF coadministration as well as *CYP2C19*\*2 carriers significantly influenced ETV CL ( $\Delta\text{OF} = -39.0$ ,  $P < 0.0001$ , in comparison with the model without any covariates), and explained altogether 16% of the variability in ETV concentrations. The final average pharmacokinetic parameters and between-participant variability are presented in Table 3. Goodness-of-fit plots of population and individual predictions obtained in the final model versus the observations are presented in (Supplementary Figure S1, <http://links.lww.com/FPC/A536>). The combination of genetic variants and comedication is shown in Fig. 1. Exploratory analysis excluding four individuals with no genotype data did not yield any differences.

### Model evaluation and assessment

The median parameter estimates obtained with bootstrap with the 95% CI are presented in Table 3. The median parameters differed in less than 10% from those obtained with the original dataset. The parameter estimates of the final population pharmacokinetic model were within the 95% CI of the bootstrap results, indicating that the model was acceptable. A bias of 3% (95% CI: –5 to 11%) was calculated applying the structural model without covariates to the external model validation dataset; the precision of the model was 62%. A similar bias of 6% (95% CI: –11 to 25%) was calculated for population predictions, with a much higher precision of 148%. The sensitivity analysis did not show any difference in the estimated pharmacokinetic and covariate effect parameters after the exclusion of data suggestive of nonadherence to treatment. Goodness-of-fit plots for the validation dataset are shown in Supplementary Figure S2 (<http://links.lww.com/FPC/A537>). The VPC of the observed concentrations versus time with the 95% prediction interval is shown in Fig. 2. Six and 3% of the data were outside the CI for the 200 mg twice daily regimen and 400 mg once daily, respectively, confirming the adequacy of the model.

**Table 3** Pharmacokinetic parameters obtained in the final model

Parameters <sup>a</sup>	Final population pharmacokinetic parameters		Bootstrap (n=200 samples)			
	Estimate	SE (%) <sup>c</sup>	Mean	SE (%) <sup>d</sup>	95% CI	Difference (%) <sup>h</sup>
CL/F (l/h)	30.3	8.6	30.0	7.6	25.5–34.5	–0.9
V <sub>d</sub> /F (l)	1374.4	41.0	1446.7	45.0	178.7–2714.8	5.0
D <sub>1</sub> (h)	2.41	33.0	2.50	29.0	1.09–3.91	3.5
θ <sub>DRV</sub> <sup>e</sup>	1.40	10.0	1.43	11.0	1.11–1.73	1.5
θ <sub>TDF</sub> <sup>f</sup>	1.42	9.1	1.44	8.8	1.19–1.69	0.8
θ <sub>CYP2C19*2</sub> <sup>g</sup>	0.77	9.9	0.78	11.0	0.62–0.95	1.6
ω (CL) (CV%) <sup>b</sup>	43.0	44.0 <sup>d</sup>	41.4	47.0	31.2–49.5	–4.1
σ (CV%) <sup>b</sup>	38.5	39.0 <sup>d</sup>	38.2	40.0	31.6–43.9	–0.7

Median and 95% confidence interval of the pharmacokinetic parameters obtained from the bootstrapped 200 ETV samples.

CI, confidence interval; CL, clearance; D<sub>1</sub>, duration of absorption; DRV, darunavir; DRVr, ritonavir-boosted darunavir; ETV, etravirine; TDF, tenofovir; V<sub>d</sub>, volume of distribution.

Final model:  $CL = \theta_1 (\theta_{DRV})^{DRV} (\theta_{TDF})^{TDF} (\theta_{CYP2C19*2})^{CYP2C19*2}$ , where DRV=0 or 1, TDF=0 or 1, and CYP2C19\*2=0 or 1.

<sup>a</sup>CL/F, mean apparent clearance; V/F, mean apparent volume of distribution; D<sub>1</sub>, mean absorption time; F, bioavailability.

<sup>b</sup>ω, estimate of interindividual variability; σ, estimate of intraindividual variability and expressed as CV (%).

<sup>c</sup>Standard errors of the estimates (SE), defined as SE/estimate and expressed as percentages.

<sup>d</sup>Standard errors of the coefficient of variation, taken as  $\sqrt{SE/estimate}$  and expressed as percentage.

<sup>e</sup>Relative influence of DRV on ETV clearance (see text).

<sup>f</sup>Relative influence of TDF on ETV clearance (see text).

<sup>g</sup>Relative influence of CYP2C19\*2 on ETV clearance (see text).

<sup>h</sup>Difference (%) = (bootstrap mean value – typical value from the final model)/bootstrap mean × 100.

## Genotyping

Among 125 SNPs genotyped, 16 failed quality control criteria for genotyping; two functional SNPs in *CYP2C9* [rs1799853 (*CYP2C9\*2*) and rs1057910 (*CYP2C9\*3*)] and one in the nuclear receptor *NR1I2* (rs7643645) were regenotyped by other techniques (see the Materials and methods section). Six SNPs were monomorphic [rs7439366, rs4987161 (*CYP3A4\*17*), rs28399504 (*CYP2C19\*4*), rs41291556 (*CYP2C19\*8*), rs72558186 (*CYP2C19\*7*), and rs1800961] in this dataset. Finally, 106 SNPs (eight SNPs in the first step and 98 in the second discovery step) were included in the study.

## Genetic discovery analysis

None of the 98 SNPs of the discovery step reached study-wide significance. Four SNPs showed nominal significance ( $P < 0.05$ ) using an additive genetic model. Three of them, rs2003569 and rs17863800, both located in the *UGT1A* locus, and rs4400059, located in intron 6 of *UGT2B11*, were associated with higher ETV CL ( $P = 7.43 \times 10^{-4}$  with  $\beta = 35.26$ ,  $9.08 \times 10^{-4}$  with  $\beta = 35$  and  $0.011$  with  $\beta = 15.60$ , respectively) (Fig. 3a). The fourth nominal association was rs2650000 ( $P = 0.015$  with  $\beta = -6.76$ ), a promoter variant of *HNF1A*. The two *UGT1A* locus variants are tSNPs in linkage disequilibrium ( $r^2 = 0.403$ ,  $D' = 1$ ). SNP rs17863800 captures rs6755571 (*UGT1A\*2*), a change of proline to threonine that is expected to have functional impact. The association of the two SNPs and ETV CL is because of one single individual homozygous for the rare allele that presented a very high ETV CL; heterozygosity was not associated with the study phenotype (Fig. 3b). This individual was

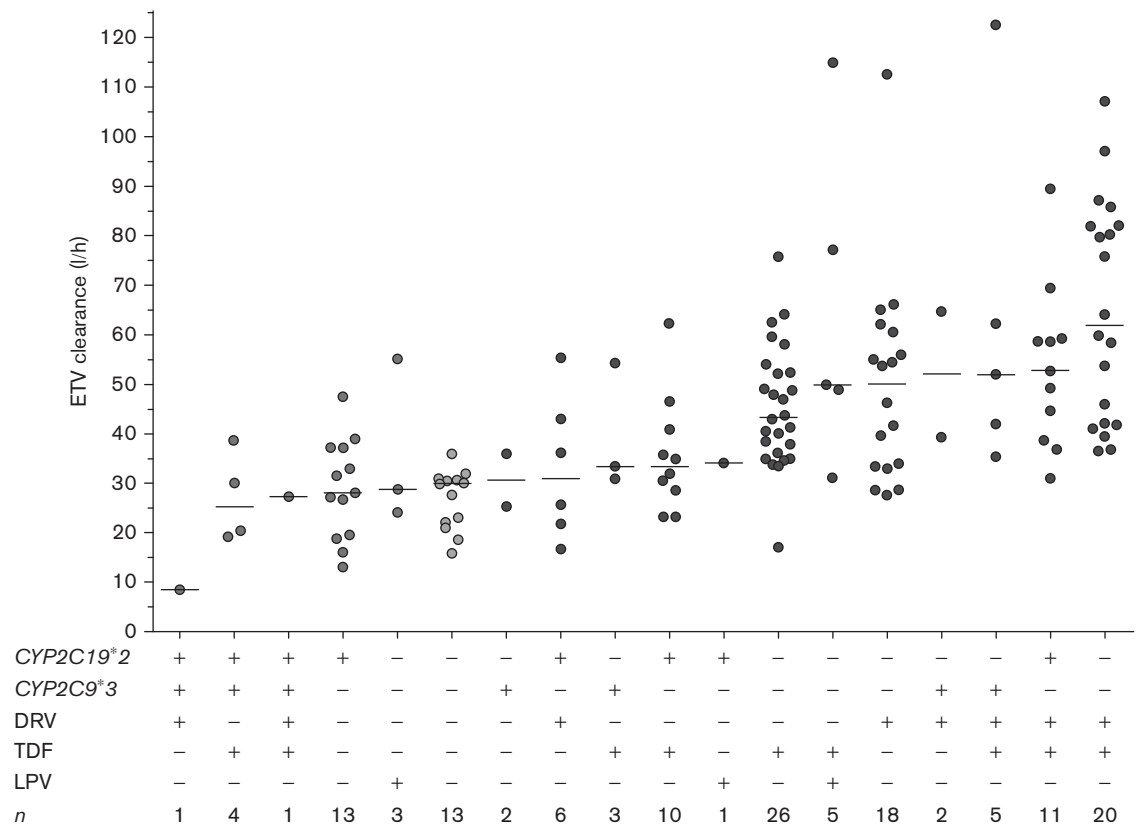
a 42-year-old heterosexual man from Sub-Saharan Africa who had three ETV plasma determinations consistently associated with plasma levels below percentile 5: 82 and 119 ng/ml after 9.5 h of 200 mg ETV BID and 181 ng/ml after 8.83 h of 300 mg ETV BID. In addition to ETV, this individual received TDF, FTC, and LPVr, achieving optimal virological control without modification of dosing.

We aimed to validate this signal by genotyping rs2003569 in a replication dataset of 64 HIV-infected individuals. We identified 46 individuals homozygous for the common allele, 18 heterozygous individuals, and none homozygous for the rare allele; therefore, the association could not be validated formally.

## Discussion

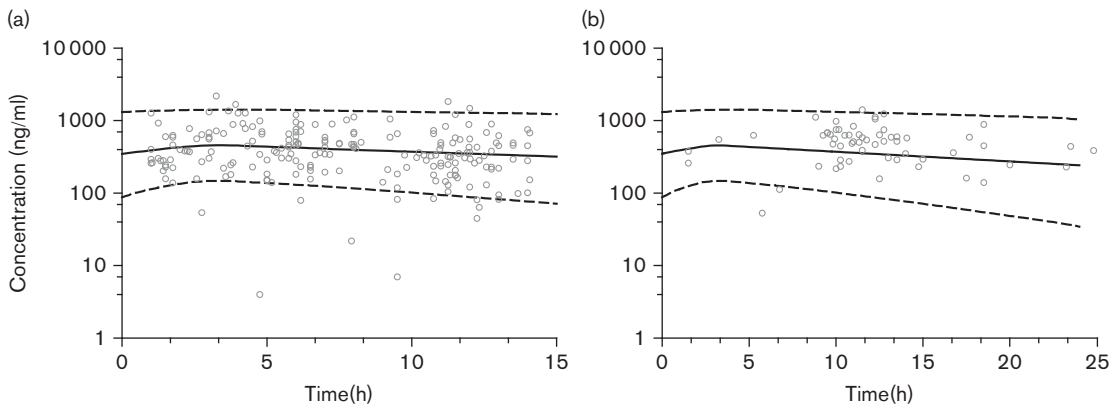
The present study confirmed the influence of several co-administered antiretroviral drugs as significant factors of ETV pharmacokinetics. It quantified the impact of genetic variants on ETV elimination and showed the opposing influences of concomitant antiretroviral drugs and genetic variants on ETV disposition. It tested the influence of new allelic variants that might affect ETV elimination. ETV was best described by a one-compartment model, with pharmacokinetics parameters in close agreement with previously reported results [7]. A high variability in drug absorption was observed, which could be attributed to the effect of food. Food intake increases ETV exposure. Scholler-Gyure *et al.* [8] reported 51% lower drug exposure when ETV was administered in the fasted state compared with administration after a standard or a high-fat breakfast. ETV exposure was 20

Fig. 1



Contribution of co-medication and functional genetic variants in *CYP2C19* and *CYP2C9* to etravirine clearance. Ordered distribution of unadjusted individual CL (baseline model) (circles) with median CL (bars) stratified by the presence of contributing genetic variants and co-medications. Each dot represents the median etravirine CL of an individual. The number of individuals in each stratum (*n*) is indicated. CL, clearance; DRV, darunavir; ETV, etravirine; LPV, lopinavir; TDF, tenofovir.

Fig. 2

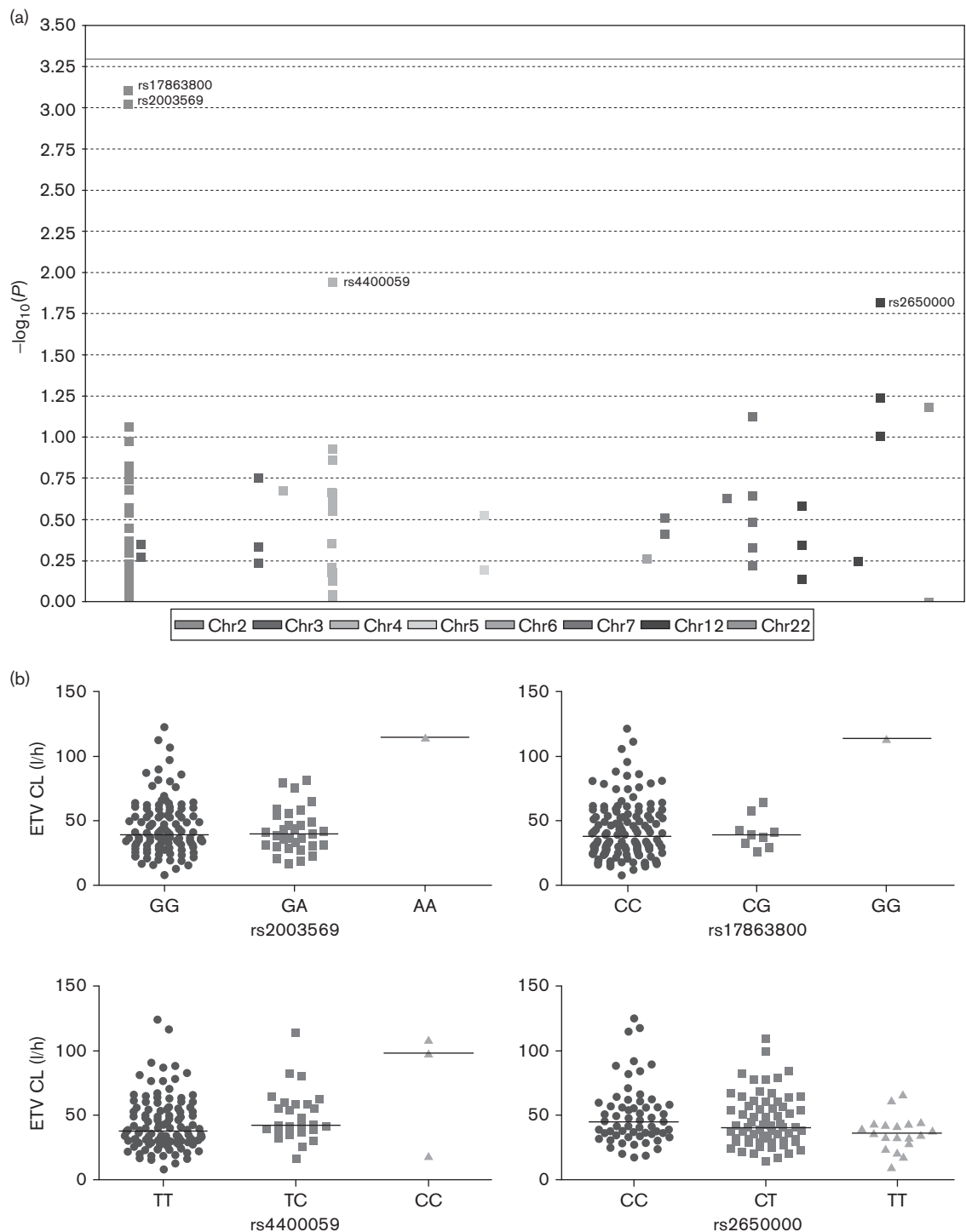


Model predictive set. Etravirine observed concentrations (open circles) versus time plots after 200 mg twice daily (a) and 400 mg once daily (b) with population predictions (solid line) and the 95% prediction interval (dotted lines).

and 25% lower after a light breakfast and a breakfast enriched with fiber, respectively. Food status was, however, not available, which is a limitation of the study.

ETV is a substrate of CYP3A4, CYP2C9, and CYP2C19, and pharmacokinetic interactions with concomitantly administered antiretroviral drugs may be expected [2,3,27].

Fig. 3



Genetic discovery analysis. (a) Manhattan plot indicating the 99 SNPs analyzed in eight chromosomes. The y-axis represents the negative log of the associated  $P$  value from the additive genetic model. The black line indicates the study-wide cutoff for significance, corresponding to Bonferroni's correction for multiple testing,  $P=5.05 \times 10^{-4}$ . None of the investigated SNPs reached study-wide significance. Four SNPs, rs17863800, rs2003569, rs4400059, and rs2650000, reached nominal significance ( $P=7.43 \times 10^{-4}$ ,  $9.08 \times 10^{-4}$ , 0.011, and 0.015, respectively). (b) Association of rs2003569, rs17863800, rs4400059, and rs2650000 with etravirine clearance. Each dot represents one individual; the median values are shown. The two *UGT1A* markers (rs2003569 and rs17863800) are in linkage disequilibrium,  $r^2=0.342$  and  $D'=1$ ; however, the signal corresponds to a single individual with both minor variants in homozygosis. rs4400059 is an intronic SNP in *UGT2B11* gene and rs2650000 is a promoter SNP of *HNF1A* gene. CL, clearance; ETV, etravirine; SNP, single-nucleotide polymorphism.



In agreement with previous findings [7,28–30], we found that DRVr and TDF increased ETV CL by 40 and 42%, respectively. The mechanisms for these interactions are not fully elucidated. Scholler-Gyure *et al.* [30] hypothesized that interaction with DRVr may be through induction of CYP2C9, CYP2C19, and UGTs by ritonavir. Kakuda *et al.* [29] discussed a possible interaction with TDF that would involve CYP1A1. TDF could induce CYP1A, and in-vitro data suggest that CYP1A1 play a role in ETV metabolism. ETV is not a substrate of any of the known ABC transporters [5]. Although not statistically significant, we observed a 40% increase in ETV CL under LPVr treatment as reported by the manufacturer [31]. Most probably, the effect did not reach statistical significance because of the small number of individuals ( $n = 9$ ) receiving this drug. Overall, interactions with these various drugs may not affect ETV elimination to a clinically relevant extent [31]; however, this may merit additional investigation.

None of the demographic covariates significantly affected ETV CL, in agreement with previous reports [7]. We did not observe an effect of comedications such as antifungal azoles or antacids on ETV CL as reported previously [4,24,32]. This may be because of the low number of participants taking these drugs. We did not observe an effect of hepatitis C coinfection on ETV CL. One study found a slight increase in ETV exposure in individuals coinfecting with hepatitis C [7]; however, no dose adjustment was required according to the manufacturer [31].

There is increasing evidence on the importance of genetic testing of *CYP2C9* and *CYP2C19* to predict drug CL and to perform dosage adjustment of many drugs [33]. *CYP2C19\*2*, *CYP2C9\*3* are associated with decreased enzyme activity and affect the CL and clinical response of several drugs such as warfarin and clopidogrel [34–36]. A reduction in ETV CL was observed in LOF carriers of rs4244285 (*CYP2C19\*2*). Although not statistically significant, LOF carriers of rs1057910 (*CYP2C9\*3*) showed a similar reduction in CL. The lack of statistical significance might be related to either power issues because of the limited number of individuals carrying this allele ( $n = 18$ ) or the fact that most of the carriers of *CYP2C9\*3* ( $n = 16$ ) had concomitant TDF and/or DRVr that mask the influence of this allele. Altogether, the genetic effect was of a limited magnitude; it accounted for 5% of the variability in ETV CL, which might not exert a clinically significant impact.

We attempted to discover new variants in a set of 31 candidate genes that might influence ETV metabolism. None of the variants reached study-wide significance. A single individual homozygous for *UGT1A4\*2* (rs6755571) presented very high ETV CL. This variant has been associated with decreased glucuronidation activity of  $\beta$ -naphthylamine and dihydrotestosterone [37], higher activity against an active metabolite of nitrosamine [38],

and no change in activity against tamoxifen [39] or tacrolimus [40]. Heterozygosity was not associated with ETV CL, and we did not identify additional homozygous individuals in an independent population. In the future, if other individuals are identified, this allele would require functional investigation.

## Conclusion

This study used a population pharmacokinetic approach to identify the potential factors influencing ETV disposition. The model showed the effects of concomitant antiretroviral drugs and genetic variants on ETV CL that explained altogether 16% of the variance in ETV levels, leaving a large fraction unexplained at the population level.

## Acknowledgements

C.C. and A.T.: conceived and designed the experiments; M.R., R.M., and J.D.L.: carried out the genetic analyses; A.F.-M. and L.A.D.: therapeutic drug monitoring; R.L., M.A.-A., M.G., T.B., and C.C.: population pharmacokinetic analysis; R.L., M.A.-A., and M.G.: analyzed data; M.C., H.F.G., H.F., C.M., E.B., and A.C.: organized the clinical cohort and provided samples; all authors: reviewed the manuscript for important intellectual content and approved the final version; M.A.-A., M.R., C.C., and A.T.: wrote the paper.

The authors thank the Vital-IT Platform for high-performance computing of the Swiss Institute of Bioinformatics for providing the support for the population pharmacokinetic analyses. They thank the patients who participated in the SHCS, the physicians and study nurses for excellent patient care, Martin Rickenbach, Franziska Schöni-Affolter, and Yannick Vallet from the SHCS Data Center in Lausanne for the data management, and Marie-Christine Francioli for administrative assistance.

The members of the Swiss HIV Cohort Study (SHCS) are J. Barth, M. Battegay, E. Bernasconi, J. Böni, H.C. Bucher, C. Burton-Jeangros, A. Calmy, M. Cavassini, C. Cellera, M. Egger, L. Elzi, J. Fehr, J. Fellay, M. Flepp, P. Francioli (President of the SHCS), H. Furrer (Chairman of the Clinical and Laboratory Committee), C.A. Fux, M. Gorgievski, H. Günthard, D. Haerry (Deputy of 'Positive Council'), B. Hasse, H.H. Hirsch, B. Hirschel, I. Hösli, C. Kahlert, L. Kaiser, O. Keiser, C. Kind, T. Klimkait, H. Kovari, B. Ledergerber, G. Martinetti, B. Martinez de Tejada, K. Metzner, N. Müller, D. Nadal, G. Pantaleo, A. Rauch (Chairman of the Scientific Board), S. Regenass, M. Rickenbach (Head of Data Center), C. Rudin (Chairman of the Mother & Child Substudy), P. Schmid, D. Schultze, F. Schöni-Affolter, J. Schüpbach, R. Speck, P. Taffé, P. Tarr, A. Telenti, A. Trkola, P. Vernazza, R. Weber, S. Yerly.

This work was supported by the Swiss National Science Foundation (SNF Grant #324730-124943) and in the framework of the Swiss HIV Cohort Study (SNF Grant #33CS30-134277).

## Conflicts of interest

There are no conflicts of interest.

## References

- Andries K, Azijn H, Thielemans T, Ludovici D, Kukla M, Heeres J, *et al.* TMC125, a novel next-generation nonnucleoside reverse transcriptase inhibitor active against nonnucleoside reverse transcriptase inhibitor-resistant human immunodeficiency virus type 1. *Antimicrob Agents Chemother* 2004; **48**:4680–4686.
- Dickinson L, Khoo S, Back D. Pharmacokinetic evaluation of etravirine. *Expert Opin Drug Metab Toxicol* 2010; **6**:1575–1585.
- Scholler-Gyure M, Kakuda TN, Raoof A, De Smedt G, Hoetelmans RM. Clinical pharmacokinetics and pharmacodynamics of etravirine. *Clin Pharmacokinet* 2009; **48**:561–574.
- Kakuda TN, Scholler-Gyure M, Hoetelmans RM. Pharmacokinetic interactions between etravirine and non-antiretroviral drugs. *Clin Pharmacokinet* 2011; **50**:25–39.
- Zembruski NC, Haefeli WE, Weiss J. Interaction potential of etravirine with drug transporters assessed in vitro. *Antimicrob Agents Chemother* 2011; **55**:1282–1284.
- Kakuda TN, Scholler-Gyure M, Hoetelmans RM. Clinical perspective on antiretroviral drug–drug interactions with the non-nucleoside reverse transcriptase inhibitor etravirine. *Antivir Ther* 2010; **15**: 817–829.
- Kakuda TN, Wade JR, Snoeck E, Vis P, Scholler-Gyure M, Peeters MP, *et al.* Pharmacokinetics and pharmacodynamics of the non-nucleoside reverse-transcriptase inhibitor etravirine in treatment-experienced HIV-1-infected patients. *Clin Pharmacol Ther* 2010; **88**:695–703.
- Scholler-Gyure M, Boffito M, Pozniak AL, Leemans R, Kakuda TN, Woodfall B, *et al.* Effects of different meal compositions and fasted state on the oral bioavailability of etravirine. *Pharmacotherapy* 2008; **28**:1215–1222.
- Fayet Mello A, Buclin T, Franc C, Colombo S, Cruchon S, Guignard N, *et al.* Cell disposition of raltegravir and newer antiretrovirals in HIV-infected patients: high inter-individual variability in raltegravir cellular penetration. *J Antimicrob Chemother* 2011; **66**:1573–1581.
- Fayet A, Beguin A, Zanolari B, Cruchon S, Guignard N, Telenti A, *et al.* A LC-tandem MS assay for the simultaneous measurement of new antiretroviral agents: raltegravir, maraviroc, darunavir, and etravirine. *J Chromatogr B Analyt Technol Biomed Life Sci* 2009; **877**:1057–1069.
- FDA. *Guidance for industry: bioanalytical method validation 2001*. Silver Spring, MD: FDA; 2012.
- Menard V, Eap O, Harvey M, Guillemette C, Levesque E. Copy-number variations (CNVs) of the human sex steroid metabolizing genes UGT2B17 and UGT2B28 and their associations with a UGT2B15 functional polymorphism. *Hum Mutat* 2009; **30**:1310–1319.
- Blaisdell J, Jorge-Nebert LF, Coulter S, Ferguson SS, Lee SJ, Chanas B, *et al.* Discovery of new potentially defective alleles of human CYP2C9. *Pharmacogenetics* 2004; **14**:527–537.
- Dai D, Zeldin DC, Blaisdell JA, Chanas B, Coulter SJ, Ghanayem BI, *et al.* Polymorphisms in human CYP2C8 decrease metabolism of the anticancer drug paclitaxel and arachidonic acid. *Pharmacogenetics* 2001; **11**: 597–607.
- De Morais SM, Wilkinson GR, Blaisdell J, Meyer UA, Nakamura K, Goldstein JA. Identification of a new genetic defect responsible for the polymorphism of (S)-mephenytoin metabolism in Japanese. *Mol Pharmacol* 1994; **46**: 594–598.
- Ferguson RJ, de Morais SM, Benhamou S, Bouchardy C, Blaisdell J, Ibeanu G, *et al.* A new genetic defect in human CYP2C19: mutation of the initiation codon is responsible for poor metabolism of S-mephenytoin. *J Pharmacol Exp Ther* 1998; **284**:356–361.
- Ibeanu GC, Blaisdell J, Ferguson RJ, Ghanayem BI, Brosen K, Benhamou S, *et al.* A novel transversion in the intron 5 donor splice junction of CYP2C19 and a sequence polymorphism in exon 3 contribute to the poor metabolizer phenotype for the anticonvulsant drug S-mephenytoin. *J Pharmacol Exp Ther* 1999; **290**:635–640.
- Sim SC, Risinger C, Dahl ML, Aklilu E, Christensen M, Bertilsson L, *et al.* A common novel CYP2C19 gene variant causes ultrarapid drug metabolism relevant for the drug response to proton pump inhibitors and antidepressants. *Clin Pharmacol Ther* 2006; **79**:103–113.
- Kuehl P, Zhang J, Lin Y, Lamba J, Assem M, Schuetz J, *et al.* Sequence diversity in CYP3A promoters and characterization of the genetic basis of polymorphic CYP3A5 expression. *Nat Genet* 2001; **27**:383–391.
- Perera MA. The missing linkage: what pharmacogenetic associations are left to find in CYP3A? *Expert Opin Drug Metab Toxicol* 2010; **6**:17–28.
- De Bakker PI, Yelensky R, Pe'er I, Gabriel SB, Daly MJ, Altshuler D. Efficiency and power in genetic association studies. *Nat Genet* 2005; **37**:1217–1223.
- Menard V, Girard H, Harvey M, Perusse L, Guillemette C. Analysis of inherited genetic variations at the UGT1 locus in the French-Canadian population. *Hum Mutat* 2009; **30**:677–687.
- Balding DJ. A tutorial on statistical methods for population association studies. *Nat Rev Genet* 2006; **7**:781–791.
- Kakuda TN, Van Solingen-Ristea R, Aharchi F, De Smedt G, Witek J, Nijs S, *et al.* Pharmacokinetics and short-term safety of etravirine in combination with fluconazole or voriconazole in HIV-negative volunteers. *J Clin Pharmacol* 2012; **XX**:1–10.
- Sheiner LB, Beal SL. Some suggestions for measuring predictive performance. *J Pharmacokinet Biopharm* 1981; **9**:503–512.
- Purcell S, Neale B, Todd-Brown K, Thomas L, Ferreira MA, Bender D, *et al.* PLINK: a tool set for whole-genome association and population-based linkage analyses. *Am J Hum Genet* 2007; **81**:559–575.
- Brown KC, Paul S, Kashuba AD. Drug interactions with new and investigational antiretrovirals. *Clin Pharmacokinet* 2009; **48**:211–241.
- Boffito M, Winston A, Jackson A, Fletcher C, Pozniak A, Nelson M, *et al.* Pharmacokinetics and antiretroviral response to darunavir/ritonavir and etravirine combination in patients with high-level viral resistance. *Aids* 2007; **21**:1449–1455.
- Kakuda TN, Scholler-Gyure M, De Smedt G, Beets G, Aharchi F, Peeters MP, *et al.* Assessment of the steady-state pharmacokinetic interaction between etravirine administered as two different formulations and tenofovir disoproxil fumarate in healthy volunteers. *HIV Med* 2009; **10**:173–181.
- Scholler-Gyure M, Kakuda TN, Sekar V, Woodfall B, De Smedt G, Lefebvre E, *et al.* Pharmacokinetics of darunavir/ritonavir and TMC125 alone and coadministered in HIV-negative volunteers. *Antivir Ther* 2007; **12**:789–796.
- Tibotec. *Intelligence. Highlights of prescribing information*. NJ, USA: Tibotec; 2011.
- Scholler-Gyure M, Kakuda TN, De Smedt G, Vanaken H, Bouche MP, Peeters M, *et al.* A pharmacokinetic study of etravirine (TMC125) co-administered with ranitidine and omeprazole in HIV-negative volunteers. *Br J Clin Pharmacol* 2008; **66**:508–516.
- Zhou SF, Zhou ZW, Huang M. Polymorphisms of human cytochrome P450 2C9 and the functional relevance. *Toxicology* 2010; **278**:165–188.
- Johansson I, Ingelman-Sundberg M. Genetic polymorphism and toxicology – with emphasis on cytochrome p450. *Toxicol Sci* 2011; **120**:1–13.
- Simon T, Bhatt DL, Bergougnan L, Farenc C, Pearson K, Perrin L, *et al.* Genetic polymorphisms and the impact of a higher clopidogrel dose regimen on active metabolite exposure and antiplatelet response in healthy subjects. *Clin Pharmacol Ther* 2011; **90**:287–295.
- Tatarunas V, Lesauskaite V, Veikutiene A, Jakuska P, Benetis R. The influence of CYP2C9 and VKORC1 gene polymorphisms on optimal warfarin doses after heart valve replacement. *Medicina (Kaunas)* 2011; **47**:25–30.
- Ehmer U, Vogel A, Schutte JK, Krone B, Manns MP, Strassburg CP. Variation of hepatic glucuronidation: novel functional polymorphisms of the UDP-glucuronosyltransferase UGT1A4. *Hepatology* 2004; **39**:970–977.
- Wiener D, Fang JL, Dossett N, Lazarus P. Correlation between UDP-glucuronosyltransferase genotypes and 4-(methylnitrosamino)-1-(3-pyridyl)-1-butanone glucuronidation phenotype in human liver microsomes. *Cancer Res* 2004; **64**:1190–1196.
- Sun D, Chen G, Dellinger RW, Duncan K, Fang JL, Lazarus P. Characterization of tamoxifen and 4-hydroxytamoxifen glucuronidation by human UGT1A4 variants. *Breast Cancer Res* 2006; **8**:R50.
- Laverdiere I, Caron P, Harvey M, Levesque E, Guillemette C. In vitro investigation of human UDP-glucuronosyltransferase isoforms responsible for tacrolimus glucuronidation: predominant contribution of UGT1A4. *Drug Metab Dispos* 2011; **39**:1127–1130.